

OBSERVATIONS OF [C I] AND CO ABSORPTION IN COLD, LOW-DENSITY CLOUD MATERIAL TOWARD THE GALACTIC CENTER BROAD-LINE EMISSION

J. STAGUHN,¹ J. STUTZKI,¹ R. A. CHAMBERLIN,^{2,3} S. P. BALM,^{4,5} A. A. STARK,⁴ A. P. LANE,⁴
R. SCHIEDER,¹ AND G. WINNEWISSER¹

Received 1996 November 7; accepted 1997 July 23

ABSTRACT

We report the detection of a deep ${}^3P_1 \rightarrow {}^3P_0$ (C I) absorption feature at $v_{\text{LSR}} = 12 \text{ km s}^{-1}$ with a line width of 6 km s^{-1} toward extended line emission at a distance of $11'$ from Sgr C. The 492 GHz observations were made with the Antarctic Submillimeter Telescope and Remote Observatory. The absorption feature allows the derivation of lower limits for the C I column density in the cold foreground material. The feature is unlikely to be caused by self-absorption within the [C I]-emitting cloud because it is observed over a region at least $4'$ across and is also seen in emission $22'$ north of the Galactic plane in ${}^{12}\text{CO } J = 2-1$. In order to determine the temperature and the abundance ratio of C I to CO in the foreground gas, we compare the observations with ${}^{12}\text{CO}$ and ${}^{13}\text{CO } J = 1-0$ observations obtained with the Bell Labs 7 m antenna and with ${}^{12}\text{CO}$ and ${}^{13}\text{CO } J = 2-1$ observations made with the Kölner Observatorium für Submillimeter und Millimeter Astronomie 3 m telescope. All these observations have about the same beam size. On the assumption that the background emission is not spatially associated with the absorbing cloud(s), a consistent model for the observed line intensities yields an excitation temperature of 3.5 K for ${}^{13}\text{CO}$ and 5 K for [C I], which implies low volume densities, $n(\text{H}_2) \lesssim 10^3 \text{ cm}^{-3}$. The measured abundance ratio of C I to ${}^{13}\text{CO}$ is ~ 34 . This value is consistent with photochemical model calculations that predict an abundance ratio of C I to ${}^{12}\text{CO}$ of ~ 1 and a ${}^{12}\text{CO}$ to ${}^{13}\text{CO}$ ratio of ~ 30 (reduced in comparison to the intrinsic ${}^{12}\text{C}$ to ${}^{13}\text{C}$ isotopic ratio of 60 by fractionation). The observed ${}^{13}\text{CO}$ column density corresponds to an A_V of 4.6 mag, i.e., the hydrogen column density $N(\text{H})$ is $\sim 9 \times 10^{21} \text{ cm}^{-2}$. This, together with the observed [C I] line width, indicates that the absorption is likely due to several translucent clouds.

We compare our results with line fluxes derived from the large-scale, low-resolution COBE FIRAS spectral line survey of [C I] ${}^3P_1 \rightarrow {}^3P_0$ and [C I] ${}^3P_2 \rightarrow {}^3P_1$ emission in the Galactic plane. Taking into account beam filling, the lower limit for the column density of cold ($T_{\text{ex}} \leq 10 \text{ K}$) C I that is traced by our absorption observations is at least a factor of 2 higher than the column density of the warmer C I ($T_{\text{ex}} \geq 20 \text{ K}$) detected in emission by COBE. Our results suggest that a substantial fraction of atomic carbon in the interstellar medium may be difficult to detect in [C I] emission, owing to its low excitation.

Subject headings: Galaxy: abundances — Galaxy: center — ISM: atoms — ISM: general — ISM: molecules — radio lines: ISM

1. INTRODUCTION

Abundance measurements of atomic carbon in translucent and dark clouds provide an important test of chemical model calculations. Observations of atomic carbon (C I) have been made mostly toward dense photodissociation regions (PDRs), in which UV fields are enhanced by several orders of magnitude compared to the general interstellar radiation field. Chemical model calculations of such PDRs agree well with observations, if a high degree of clumpiness of the cloud material is assumed (Stutzki et al. 1988; Meixner & Tielens 1993). The model calculations are very sensitive to changes in the physical parameters for clouds in

which carbon is being transformed into CO (van Dishoeck & Black 1988, 1989; Flower et al. 1994). This transformation occurs in translucent ($A_V \approx 1-5 \text{ mag}$) and low-density dark ($A_V \gtrsim 5 \text{ mag}$) clouds. Until recently, only a few C I observations toward such clouds have been made. Strong constraints on the C I to CO abundance ratio were derived from observations of eight translucent clouds by Ingalls et al. (1997), for the translucent cloud toward HD 210121 by Stark & van Dishoeck (1994), and toward MBM12 by Ingalls et al. (1994). Abundances in dense dark clouds were derived from observations by Phillips & Huggins (1981), Schilke et al. (1995), and Stark et al. (1996). In all these cases, C I was observed in emission. As the optical depth was not determined for these emission-line measurements, the derived column densities are uncertain, and excitation models must be invoked for the interpretation.

Absorption measurements of a foreground cloud toward a strong continuum or a broad-line background source give direct constraints on the physical characteristics of the absorbing gas. They are a common tool at centimeter wavelengths, where extended continuum emission can be found over wide areas of the sky. There are large-scale 21 cm [H I] surveys toward the Galactic center (see, e.g., Hagen, Lilley, & McCain 1955; Lasenby, Lasenby, & Yusef-Zadeh 1989)

¹ Universität zu Köln, I. Physikalisches Institut, Zùlpicher Strasse 77, 50937 Köln, Germany; staguhn@ph1.uni-koeln.de, stutzki@ph1.uni-koeln.de, schieder@ph1.uni-koeln.de, winnewisser@ph1.uni-koeln.de.

² Astronomy Department, Boston University, 725 Commonwealth Avenue, Boston, MA 02215; cham@bu.edu.

³ California Institute of Technology, Submillimeter Observatory, 111 Nowelo Street, Hilo, HI 96720; cham@ulu.submm.caltech.edu.

⁴ Harvard-Smithsonian Center for Astrophysics, 60 Garden Street, Cambridge, MA 02138; aas@cfa.harvard.edu, adair@cfa.harvard.edu.

⁵ Department of Physics and Astronomy, 8971 Math Sciences Building, University of California, Los Angeles, Los Angeles, CA 90095-1562; balm@astro.ucla.edu.

and absorption measurements in other species such as OH (Goss 1967) and formaldehyde (Snyder et al. 1969). These and CO observations toward Sgr A by Liszt, Sanders, & Burton (1975) show strong absorption lines near $v_{\text{LSR}} = 0$ km s⁻¹ toward the Galactic center. From the narrow line widths, the low velocities with respect to the LSR, and the depth of these features, it is concluded that the absorbing clouds are not situated in the Galactic center region and that the cloud temperatures must be very low.

As is the case for the millimeter-wave transitions of CO, there is no bright, extended continuum emission in the submillimeter. The strong, broad spectral line emission from the Galactic center, however, provides a suitable background source for absorption measurements. Our spectra toward the Galactic center have sufficient a signal-to-noise ratio to derive, for the first time, [C I] optical depths in a cold molecular cloud by absorption measurements.

2. OBSERVATIONS

The 1.7 m diameter telescope of the Antarctic Submillimeter Telescope and Remote Observatory (AST/RO) was installed during austral summer 1994–1995 at the Amundsen-Scott South Pole Station and began operations in 1995 February (Lane & Stark 1996; Stark et al. 1997). The telescope efficiency at 492 GHz was derived from a combination of skydips and Moon observations. We adopt $\eta_{\text{mb}} = 0.75$ for the 1995 data and $\eta_{\text{mb}} = 0.81$ for the 1996 data as the efficiency factor relating the receiver calibration to the temperature scale in the main beam (Chamberlin, Lane, & Stark 1997). The beam size (FWHM) was 147". The quasi-optical 492 GHz SIS receiver (Zmuidzinas & Le Duc 1993; Engargiola, Zmuidzinas, & Lo 1994) has $T_{\text{rec}} \approx 180$ K DSB. System temperatures in 1995 April ranged between 4800 and 5100 K. During the observations in 1995 October, the system temperatures varied between 1400 and 2300 K. The back end was an acousto-optical spectrometer (AOS) with 1.07 MHz resolution and 1.1 GHz bandwidth. The atmospheric transmission was checked regularly by skydip measurements and sky temperature measurements in the direction of the source. The observations were done in the position-switched mode with two reference positions, 1° away from the source in right ascension for the April observations. The October observations were made using a reference position 2° away from the Galactic plane in a region known to be free of CO emission (offset from source position: $\Delta\text{R.A.} = -120'$, $\Delta\text{decl.} = -32.5'$). A more extended region around the position of the absorption feature was observed in the 1996 winter season with the same receiver. These observations were made with the same reference positions as the 1995 April observations but were corrected for possible emission in the reference by adding a fit to the residuals between the 1995 April and October observations. Owing to problems tuning the local oscillator, these observations were made in the upper sideband rather than the more preferable lower sideband tuning used for the 1995 observations. (The intermediate frequency of the receiver is 1.5 GHz.) Typical system temperatures for these observations ranged between 4000 and 5000 K. As a conservative approach, we assume the absolute calibration to be better than 30%.

A ¹³CO (1–0) spectrum in the direction we observed in C I was obtained from the Bell Labs Galactic center observations of Bally et al. (1987), and a ¹²CO (1–0) spectrum was similarly obtained with the Bell Labs 7 m telescope (Bally

1996). The Bell Labs data were corrected for a main-beam efficiency, η_{mb} , of 0.89.

The ¹²CO (2–1) and ¹³CO (2–1) data were obtained with the Kölner Observatorium für Submillimeter und Millimeter Astronomie (KOSMA) 3 m telescope (Winnewisser et al. 1986) in 1995 November and 1996 January with a dual-channel SIS receiver. The back end for the ¹²CO (2–1) observations was an AOS with a bandwidth of 250 MHz and a resolution of 270 kHz. The back end for the ¹³CO observations was an AOS with 1.1 GHz bandwidth and a resolution of 1.07 MHz. The mean system temperature for these observations was 290 K double sideband. For the KOSMA data, we used a value of $\eta_{\text{mb}} = 0.73$, which was interpolated from the measured coupling to Jupiter and to the Moon. The observing mode was balanced position-switching with two reference positions 2° from the Galactic plane. The KOSMA pointing accuracy is $\sim 10''$ rms. Calibration for atmospheric transparency was made following a modified chopper-wheel calibration procedure (Röhrig 1995). The absolute calibration of the KOSMA telescope is accurate to within 20% as checked by careful comparison among various telescopes (Bensch et al. 1997). The relative calibration with the set of observations presented here was checked regularly on a calibration position in ρ Oph and was found to be stable within the 15% limits.

The HCO⁺ (1–0) (89.19 GHz) observations were made with the 15 m Swedish-ESO Submillimeter Telescope⁶ (SEST) in 1995 March (Staguhn et al. 1997). The observations were performed with the facility 3 mm dual-mixer Schottky receiver using mixer B, which is optimized ($T_{\text{rec}} = 280$ K single sideband) for the lower frequency range of the receiver. The SEST main-beam efficiency, η_{mb} , at this frequency is 0.75, and the beam size is 55" (FWHM). The typical system temperature during the observing session was ~ 450 K. The pointing accuracy was checked regularly by centering on the SiO maser toward AH Sco and by centering on IRAS 15194, which was also used as a relative line calibrator. The pointing was accurate within 5" limits; the relative calibration was stable within 10% limits.

3. RESULTS

Figure 1 presents the [C I] ³P₁ → ³P₀ spectrum we observed toward the position R.A. (1950) = 17^h41^m23^s.66, decl. (1950) = –29°14'22".00 at a distance of 11' from Sgr C. A deep dip at $v_{\text{LSR}} = 12$ km s⁻¹ is seen against the bright Galactic center [C I] emission. The broad, flat background emission, together with the velocity distribution of Galactic center clouds, makes it likely that this feature is caused by absorption in a foreground cloud rather than by a lack of emission from the Galactic center at this particular velocity. The detection of emission at this velocity in the HCO⁺ (1–0) line (Fig. 2) further supports this interpretation. The HCO⁺ (1–0) spectrum shown in Figure 2 was generated by positionally averaging the SEST observations to the resolution of the AST/RO main beam toward the same position. A main difference between absorption observations toward broad-line emission as presented here and spectral line absorption observations toward continuum sources becomes evident: owing to HCO⁺'s high dipole moment of 3.3 D, compared to 0.11 D for CO, the ratio of

⁶ The SEST telescope is operated by the Swedish National Facility for Radio Astronomy, Onsala Space Observatory and by ESO.

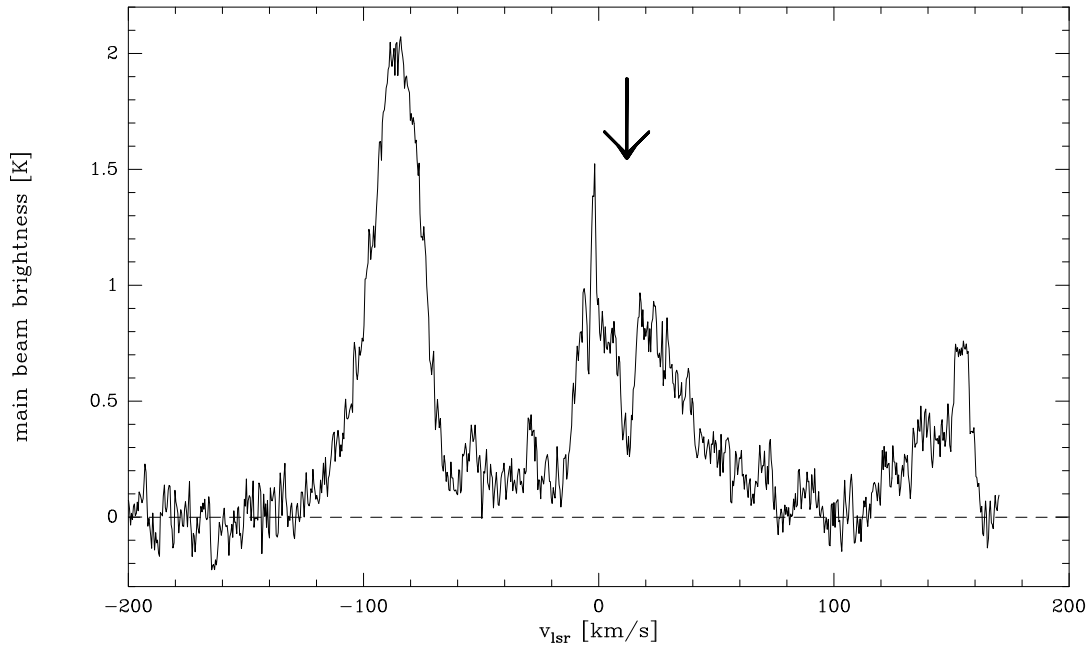


FIG. 1.—The 492 GHz [C I] $^3P_1 \rightarrow ^3P_0$ spectrum obtained with the AST/RO telescope at the position R.A. (1950) = $17^{\text{h}}41^{\text{m}}23^{\text{s}}.66$, decl. (1950) = $-29^{\circ}14'22''.00$, co-added from both the 1995 April and October observations. The absorption feature is centered at $v_{\text{LSR}} = 12 \text{ km s}^{-1}$.

the Einstein A -coefficients of HCO^+ (1–0) and ^{13}CO (1–0) is about 500, which is higher than the inverse ratio of the interstellar abundance of the two molecules (about 200; see, e.g., van Dishoeck et al. 1993). Thus HCO^+ is expected to

have a higher optical depth in its ground state than ^{13}CO (eq. [8]). This is the reason that HCO^+ (1–0) is observed in absorption toward continuum sources in a large number of cold molecular clouds—often even stronger than

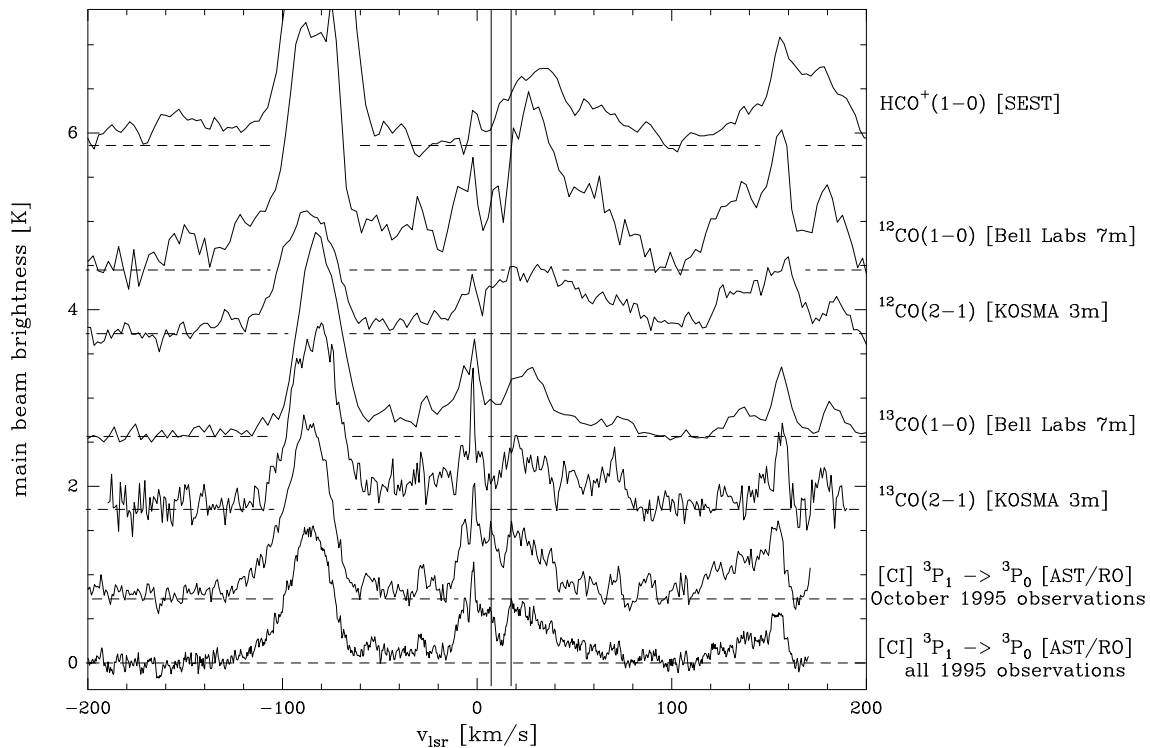


FIG. 2.—Spectra of all observed transitions at the position R.A. (1950) = $17^{\text{h}}41^{\text{m}}23^{\text{s}}.66$, decl. (1950) = $-29^{\circ}14'22''.00$. The temperature scale is appropriate for the two C I spectra at the bottom. The HCO^+ $J = 1-0$ spectrum represents an observation with the *same* angular resolution to that of the AST/RO beam at 492 GHz. The HCO^+ main-beam temperature is scaled by a factor of 2.2, the ^{12}CO main-beam temperatures are scaled by a factor of 0.2, and the ^{13}CO main-beam temperatures are scaled by a factor of 0.67. The spectra are separated by (bottom to top) 0.8, 1.0, 0.8, 1.1, 0.7, and 1.8 K. The absorption feature is located between the solid lines.

TABLE 1
UPPER LIMITS TO THE EXCITATION TEMPERATURE IN THE FOREGROUND CLOUD

Transition	$T_{\text{mb, bg}} + J_{\nu}(2.7 \text{ K})^{\text{a}}$ (K)	Upper Limit $T_{\text{ex, } f}^{\text{b}}$ (K)	$T_{\text{mb, bg}} + J_{\nu}(2.7 \text{ K}) + T_{\text{absorb}}^{\text{c}}$ (K)	Upper Limit $T_{\text{ex, } f}^{\text{d}}$ (K)
$\text{HCO}^+ J = 1-0$	1.3	2.9	... ^e	...
$^{12}\text{CO } J = 1-0$	9.8	12.4	3.6	5.9
$^{12}\text{CO } J = 2-1$	2.9	7.0	... ^e	...
$^{13}\text{CO } J = 1-0$	2.3	4.4	1.6	3.6
$^{13}\text{CO } J = 2-1$	1.2	4.6	0.74	3.9
$[\text{C I}] \ ^3P_1 - \ ^3P_0$	0.87	7.1	0.30	5.4

^a Observed brightness temperatures of the Galactic center background emission, corrected for the contribution of the 2.7 K cosmic background radiation.

^b Corresponding upper limits for T_{ex} of the foreground cloud from eq. (5).

^c Observed brightness temperatures at the center of the absorption line, corrected for the contribution of the 2.7 K cosmic background radiation.

^d Corresponding upper limits for T_{ex} of the foreground cloud from eq. (6). Eqs. (5) and (6) are valid if the background emission is distributed homogeneously over the beam area.

^e The depth of the $\text{HCO}^+ J = 1-0$ and $^{12}\text{CO } J = 2-1$ absorption is too small, if present at all; the signal-to-noise ratio is too low to derive an upper limit of T_{ex} for these transitions.

$^{13}\text{CO } (1-0)$ (see, e.g. Lucas & Liszt 1994). Nevertheless owing to its high dipole moment, the excitation temperature of HCO^+ is comparably low in both the foreground cloud and in the Galactic center background clouds. High-density clumps in the Galactic center, which have densities equal to or above the critical density of $\text{HCO}^+ (1-0)$ (several 10^5 cm^{-3}), have only a small beam-filling factor. Thus only $\text{HCO}^+ (1-0)$ with excitation temperatures of less than 2.9 K (0.2 K above the temperature of the cosmic background radiation) can be observed in absorption against the

observed broad-line emission from the Galactic center clouds (eq. [5]; Table 1).

A slight difference in the depth of the $[\text{C I}]$ absorption feature between the 1995 April and October observations (Fig. 2) could result from pointing inaccuracies of the AST/RO telescope during its first season. In addition, the two reference positions used for the April observations were not checked for possible emission. For the October observations, we therefore used a single reference position known to be emission-free in CO.

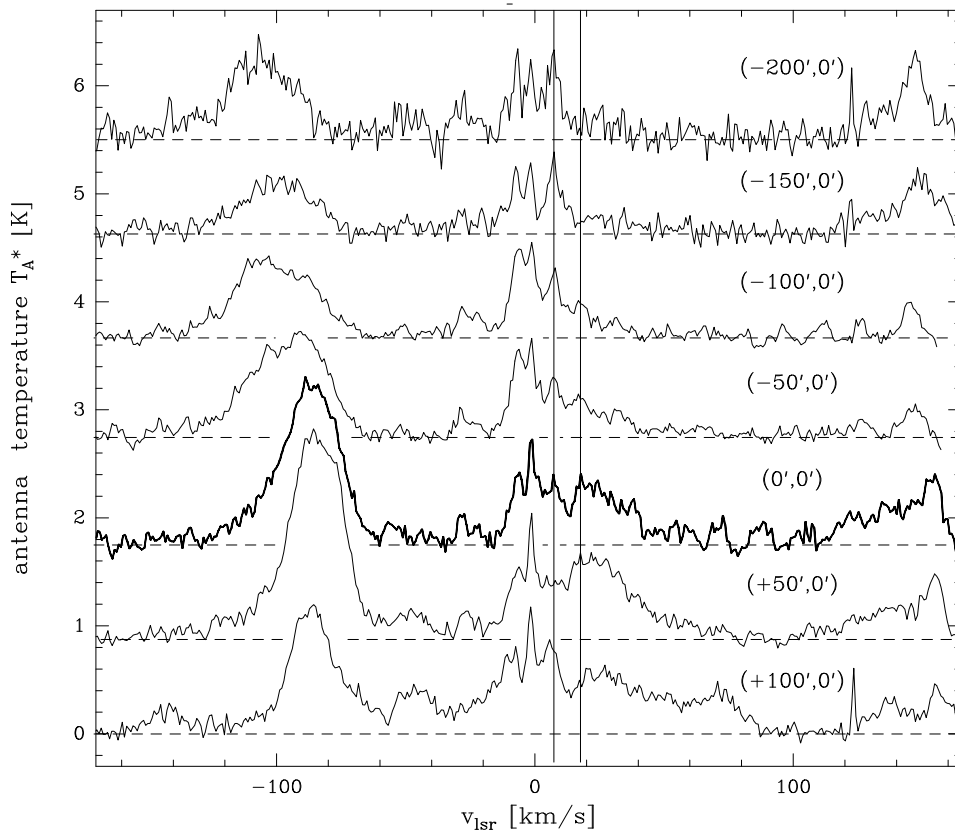


FIG. 3.—West-east cut through a 492 GHz $[\text{C I}] \ ^3P_1 \rightarrow \ ^3P_0$ map around the position of the absorption feature (*bold spectrum*) shown in Figs. 1 and 2. The angular spacing between the individual spectra is $50''$. The top two spectra and the lowest spectrum were observed with AST/RO in the 1996 winter season and show an instrumental artifact at 123 km s^{-1} . The spectra are separated by (*bottom to top*) 0.9, 0.9, 0.8, 1.0, 0.9, 1.0, and 0.9 K. The absorption feature is located between the solid lines.

Figure 3 shows [C I] spectra at 50" spacing along a west-east cut across the region. The map contains three observations obtained in the 1996 season. The absorption feature is visible in all spectra in which the background emission is sufficiently high. Note that the depth of the absorption is roughly proportional to the background emission level, which decreases toward negative R.A. offsets (as does the signal-to-noise ratio in the spectra). This strongly argues against the dip being caused by emission in the reference beam. We conclude that the absorption is spread out over a region of at least 4'. The feature cannot be caused by peculiarities in the image sideband because different sidebands were used in 1995 and 1996. The absorption feature at 12 km s⁻¹ is also present in the Bell Labs ¹²CO (1-0) and ¹³CO (1-0) spectra and in the KOSMA ¹³CO (2-1) spectrum shown in Figure 2. Channel maps showing the morphology of the ¹²CO (2-1) broad-line emission around 12 km s⁻¹ show a morphology strikingly similar to channel maps of emission at high negative velocities. This, together with its broad line width, indicates that the source of the background line emission is near the Galactic center. In a region 22' north of the Galactic plane, we observe a feature with similar velocity and width in emission in ¹²CO (2-1). In this region, almost half a degree north of the Galactic plane, the broad component of the background emission is very weak. Figure 4 shows a ¹²CO (2-1) spectrum toward the position R.A. (1950) = 17^h39^m45^s.66, decl. (1950) = -29°10'16".8. The emission line is centered at $v_{\text{LSR}} = 13.3$ km s⁻¹, with $\Delta v = 7.2$ km s⁻¹, similar to the parameters observed for the absorption feature (see Table 1). Combin-

ing all these arguments, we thus conclude that the absorption feature is not associated with the background emission sources.

3.1. Interpretation of Absorption Lines

Because of the limited resolution of the telescope, both foreground and background sources may consist of several sources within the telescope beam. We therefore consider a situation in which neither the background-emitting source nor the foreground absorbing feature fills the beam. Figure 5a shows a sketch of the situation: α_b is the filling factor of the background emission, α_f is the filling factor of the foreground source, $\alpha_{b,f}$ is the fraction of the beam area in which foreground absorption is seen against background emission, and $\alpha_{0,f}$ is the filling factor of the foreground source without background emission. The fractional area $(1 - \alpha_b - \alpha_{0,f})$ is emission free.

With these quantities, the beam-averaged intensity is

$$I_\nu = \alpha_f S_{\nu,f} (1 - e^{-\tau_{\nu,f}}) + \alpha_{b,f} I_{\nu,b} e^{-\tau_{\nu,f}} + (\alpha_b - \alpha_{b,f}) I_{\nu,b} + (1 - \alpha_b - \alpha_{0,f}) I_{\nu,2.7\text{K}} + \alpha_{0,f} I_{\nu,2.7\text{K}} e^{-\tau_{\nu,f}} + (\alpha_b - \alpha_{b,f}) I_{\nu,2.7\text{K}} e^{-\tau_{\nu,b}} + \alpha_{b,f} I_{\nu,2.7\text{K}} e^{-(\tau_{\nu,b} + \tau_{\nu,f})}, \quad (1)$$

where $S_\nu = J_\nu(T_{\text{ex}})$ is the source function, T_{ex} is the excitation temperature of the absorbing cloud, $I_{\nu,b}$ is the intensity of the quasi-continuum background, and $J_\nu(T) \equiv (h\nu/k)(e^{h\nu/kT} - 1)^{-1}$. The terms involving $I_{\nu,2.7\text{K}}$, the intensity of the 2.7 K cosmic background radiation, are negligi-

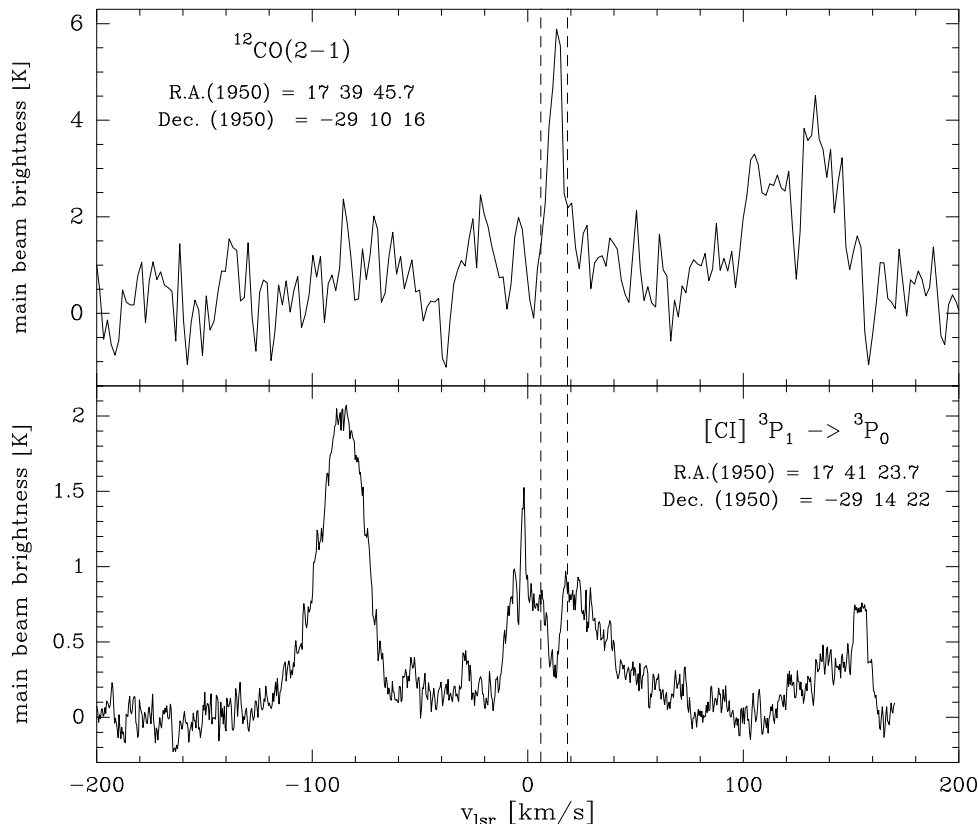


FIG. 4.—The ¹²CO $J = 2-1$ spectrum (top) toward R.A. (1950) = 17^h39^m45^s.66, decl. (1950) = -29°10'16", 22' north of the Galactic plane. The emission line is centered at $v_{\text{LSR}} = 13.3$ km s⁻¹, with $\Delta v = 7.2$ km s⁻¹, similar to the parameters observed for the 492 GHz [C I] ³P₁ → ³P₀ absorption feature at the position R.A. (1950) = 17^h41^m23^s.66, decl. (1950) = -29°14'22".00 (bottom).

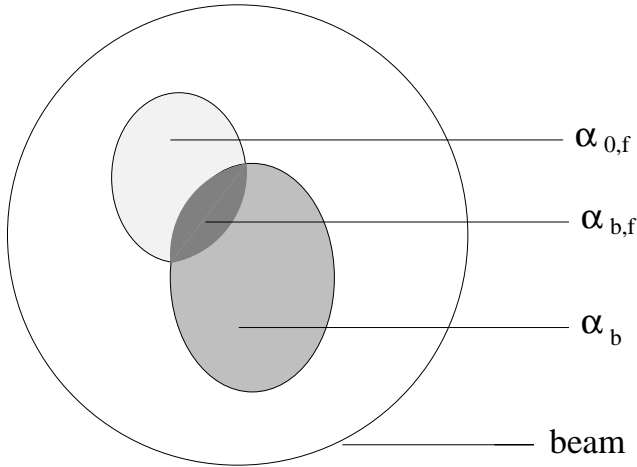


FIG. 5a

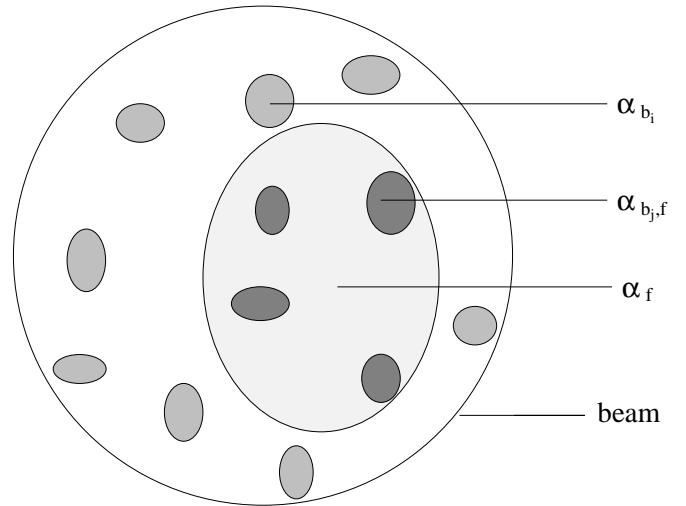


FIG. 5b

FIG. 5.—Simplified sketch to illustrate the geometrical quantities necessary to describe the emission present in one beam (*outer circle*): (a) A background cloud (with beam-filling factor α_b) is partly covered by a foreground cloud (with beam-filling factor α_f). The filling factor of the foreground source without the area covered by the background cloud is $\alpha_{0,f}$, while $\alpha_{b,f}$ is the filling factor of the overlap between background and foreground sources. (b) Sketch of the assumed observational situation in one beam: several small background sources (clumps) cover the beam area homogeneously. The filling factor of these clouds is $\alpha_b = \sum_{i=1}^n \alpha_{b,i}$.

ble for the 492 GHz [C I] observations ($J_{492\text{ GHz}}[2.7\text{ K}] = 4\text{ mK}$) but not for the lower frequencies of ^{12}CO and ^{13}CO .

The total background intensity, $I_{v,\text{bg}}$, without the absorption of a foreground cloud ($\tau_{v,f} = 0$ in eq. [1]) is

$$I_{v,\text{bg}} = \alpha_b I_{v,b} + (1 - \alpha_b) I_{v,2.7\text{ K}} + \alpha_b I_{v,2.7\text{ K}} e^{-\tau_{v,b}}. \quad (2)$$

If we assume that the background emission originates in many unresolved clumps and that the clumps are distributed *homogeneously* over the beam area (see Fig. 5b), the filling factors are related by

$$(\alpha_f - \alpha_{0,f}) = \alpha_{b,f} = \alpha_b \cdot \alpha_f. \quad (3)$$

With this assumption, and by substituting $I_{\text{absorb}} \equiv (I_v - I_{v,\text{bg}})$, we obtain the following expression for the depth of the observed absorption:

$$I_{\text{absorb}} = \alpha_f (1 - e^{-\tau_{v,f}}) [S_{v,f} - I_{v,2.7\text{ K}} - I_{v,\text{bg}}]. \quad (4)$$

We observe the foreground cloud in absorption, i.e., I_{absorb} is negative. Thus, in terms of the Rayleigh-Jeans temperature, we get

$$J_v(T_{\text{ex},f}) < T_{\text{mb,bg}} + J_v(2.7\text{ K}). \quad (5)$$

This equation gives an upper limit for the excitation temperature, T_{ex} , in the foreground cloud, independent of its (unknown) beam-filling factor, α_f .

Because $(1 - e^{-\tau_{v,f}})$ and α_f both range between 0 and 1, the constraints from equations (4) and (5) are in fact even stronger:

$$\begin{aligned} J_v(T_{\text{ex},f}) &= T_{\text{mb,bg}} + J_v(2.7\text{ K}) + \frac{T_{\text{absorb}}}{\alpha_f(1 - e^{-\tau_{v,f}})} \\ &\leq T_{\text{mb,bg}} + J_v(2.7\text{ K}) + T_{\text{absorb}}, \end{aligned} \quad (6)$$

where T_{absorb} is the (negative) antenna temperature corresponding to I_{absorb} . If $T_{\text{ex},f}$ is known, the optical depth of the foreground cloud can be calculated,

$$\tau_{v,f} = -\ln \left\{ 1 - \frac{T_{\text{absorb}}}{\alpha_f [J_v(T_{\text{ex},f}) - T_{\text{mb,bg}} - J_v(2.7\text{ K})]} \right\}, \quad (7)$$

together with the relation between optical depth and column density,

$$\tau_{v,f} = \frac{c^3 g_J A_{J,J-1} N_{J-1}}{\Delta \nu 8 \pi g_{J-1} v_{J,J-1}^3} (1 - e^{(-h\nu_{J,J-1}/kT_{\text{ex}})}), \quad (8)$$

where $A_{J,J-1}$ is the Einstein A -coefficient for spontaneous emission for the transition $J \rightarrow J-1$. The column density of a particular level (or at least a lower limit in the case $\alpha_f < 1$) can be determined using equation (8) once T_{ex} is known. We use the values of the A -coefficients of [C I] from Nussbaumer (1971); the values for the CO transitions were calculated using equation (7) in Genzel (1992).

Given the excitation temperature, $T_{\text{ex},J}$, for all relevant transition levels, we can derive the total column density, N :

$$N = \sum_J N_J = N_0 Z = N_0 \sum_J g_J \exp(-E_J/kT_{\text{ex},J}), \quad (9)$$

where E_J is the energy above the ground state ($J=0$), g_J is the statistical weight with $g_J = (2J+1)$ for rotational transitions, and Z is the partition function.

3.2. Derived Parameters

Table 1 shows the main-beam brightness temperatures of the background emission, corrected for the 2.7 K cosmic background radiation, and the brightness temperature at the peak position of the absorption feature. Also listed are the corresponding upper limits for the excitation temperature, $T_{\text{ex},f}$, of the foreground cloud (eqs. [5] and [6]). Note that the upper limits for the excitation temperature in eqs. [5] and [6] do not strongly depend on the absolute calibration accuracy of the measured antenna temperature. This is due to the large Rayleigh-Jeans temperature correction at the low excitation temperatures derived. For the millimeter transitions, the 2.7 K cosmic background emission additionally contributes to the upper limits derived for the excitation temperatures, which further reduces the relative error. To illustrate this point, we calculate the excitation temperatures for the main-beam brightness

temperatures increased by 30%, a conservative estimate for the calibration uncertainties. This results in upper limits for the excitation temperatures (Table 1, *right-hand column*) increased from 5.4 to 5.7 K for $^3P_1 \rightarrow ^3P_0$ (C I) and from 3.9 to 4.2 K for the ^{13}CO (2–1) observations. The accuracy of the derived optical depth depends on the relative depth of the absorption and thus is insensitive to the absolute calibration.

Assuming a beam-filling factor, α_f , of 1, the column densities calculated from equations (7) and (8) for the two ^{13}CO transitions (see Table 2) are consistent with equation (9) if $T_{\text{ex}} \approx 3.5$ K. Escape probability calculations yield a value of T_{ex} of 5 K for [C I] at a kinetic temperature of about 7 K for both ^{13}CO and [C I] and a volume density $n(\text{H}_2)$ in the range of several 10^2 to $1 \times 10^3 \text{ cm}^{-3}$. Typical kinetic temperatures of dark clouds range between 7 and 15 K, and thus the derived value for the absorbing cloud is at the lower end of this range.

The total column density of ^{13}CO for $T_{\text{ex}} = 3.5$ K is $1 \times 10^{16} \text{ cm}^{-2}$. Figure 2 shows that the absorption is barely visible in the ^{12}CO (2–1) spectrum. It is not possible to derive the ^{12}CO optical depth from this observation owing to the low signal-to-noise ratio, and the ^{12}CO data do not allow the calculation of an excitation temperature. If $T_{\text{ex}} = 3.5$ K for ^{12}CO , the calculated ^{12}CO column density would be $2.3 \times 10^{15} \text{ cm}^{-2}$, a value which is smaller than that derived for ^{13}CO . This is highly unlikely. The observed ^{12}CO emission probably has a T_{ex} which is different from that of the ^{13}CO , as would be expected if radiative trapping for the highly optical thick ^{12}CO lines increases T_{ex} in the warmer surface layers of the observed cloud material. Thus we will discuss only the physical parameters derived for ^{13}CO and C I. The observed parameters for these transitions and the calculated column densities are listed in Table 2. The column density calculated for C I from all observations and the value derived from the 1995 October observations agree within the errors. We will hereafter refer to the October observations, as these were observed with a reference position known to be emission free in CO.

Assuming an isotopic ratio $^{12}\text{CO}/^{13}\text{CO} \approx 70$ for a typical interstellar cloud (Penzias 1980), we derive an abundance ratio of C I to ^{12}CO of ~ 0.5 . Taking the conversion factor $N(^{13}\text{CO}) = 2.18 \times 10^{15} \text{ cm}^{-2} \text{ mag}^{-1} \times A_V$ (for $A_V < 5$) from Lada et al. (1994) and the conversion $N(\text{H}) = 1.9 \times 10^{21} \text{ cm}^{-2} \text{ mag}^{-1} \times A_V$, we derive an A_V of 4.6 mag and a hydrogen column density, $N(\text{H})$, of $9 \times 10^{21} \text{ cm}^{-2}$.

We compare our observations with the results of chemical model calculations for low-density dark clouds (Schilke et al. 1995). These authors calculate a plane-parallel model of a dark cloud with $T_{\text{kin}} = 10$ K and a density profile of $n_{\text{H}} \propto 1/z^2$, up to a limit of $n_{\text{H}} = 2 \times 10^3 \text{ cm}^{-3}$, in their “low-density model.” The standard interstellar UV field

was chosen for the calculations. Their model predicts a ^{12}CO to ^{13}CO isotopic ratio of ~ 30 due to fractionation, an important effect in low-density environments that reduces the ^{12}CO to ^{13}CO abundance ratio. In the model calculations the interstellar ^{12}C to ^{13}C isotopic abundance ratio is assumed to be 60. The C I to ^{12}CO abundance ratio is then ~ 1 for the observed cloud, in agreement with the prediction of the chemical model calculations. If we assume that all hydrogen in the cloud is molecular, and take the conversion factor $^{12}\text{CO}/\text{H}_2 \approx 1 \times 10^{-4}$ (Genzel 1992), we derive a hydrogen column density, $N(\text{H})$, of $7 \times 10^{21} \text{ cm}^{-2}$, which corresponds to an A_V of 3.6 mag.

The following estimate of the cloud’s spatial extent gives a rough idea of its size and distance. With $n(\text{H}_2) \approx 10^3 \text{ cm}^{-3}$, the thickness through the cloud is ~ 2 pc for an A_V of 4 mag. The [C I] observations shown in Figure 3 indicate that the feature is at least 4’ across. Assuming spherical geometry and that the absorption is caused by only one cloud, this implies that the cloud is no more than 2 kpc away. The detection of the feature in emission in ^{12}CO (2–1) 20’ from the position from which we observe it in absorption would imply an even shorter distance. On the other hand, the relatively broad line width of the absorption feature in comparison with most Galactic disk clouds suggests that the absorption feature might be made up of several clouds, in which case the cloud ensemble would be located somewhat farther away.

4. DISCUSSION

The most important assumption in the analysis above is that there is no spatial correlation between the background emission and the absorbing clouds. Such a correlation might occur if the absorption were produced by self-absorption near the emitting cloud. This is amenable to testing with further observations at higher resolution, but it appears to be unlikely even in the context of the current data. We have mapped the feature over an angular extent of 4’ and have observed the emission feature at the same velocity in ^{12}CO (2–1).

If self-absorption can be excluded but the background clouds are not homogeneous within the beam, the observed beam-averaged background intensity, $\alpha_b I_{\text{v,bg}}$, will not agree with the background intensity behind the foreground cloud. Galactic center clouds have typical kinetic temperatures of ~ 40 K. The observed main-beam temperatures of the broad emission lines toward the absorption feature are more than an order of magnitude weaker for all observed transitions except ^{12}CO (1–0) (see Table 1). If the line emission is not optically thin, the filling factor of the background sources (i.e., the Galactic center clouds) is small. We find only a smooth gradient of the background emission level in our [C I] map (Fig. 3). This implies a homogeneous dis-

TABLE 2
OBSERVED AND FITTED PARAMETERS FOR THE LINE ABSORPTION

Transition	v_{LSR} (km s^{-1})	Δv (km s^{-1})	τ	$N_{J_{\text{lower}}}$ (cm^{-2})
[C I] (all obs.).....	11.9 ± 0.5	5.6 ± 1.2	2.0 ± 0.4	$5.2(17) \pm 1.5(17)$
[C I] (Oct. obs.).....	12.7 ± 0.3	5.9 ± 0.8	1.2 ± 0.4	$3.5(17) \pm 1.1(17)$
$^{13}\text{CO } J = 1-0$	11.1 ± 1.6	8.9 ± 2.4	2.4 ± 0.6	$6.0(15) \pm 3.2(15)$
$^{13}\text{CO } J = 2-1$	9.3 ± 1.0	8.1 ± 2.0	1.3 ± 0.7	$4.2(15) \pm 2.5(15)$

tribution of the clumps on large scales. Inhomogeneities become relevant only when the foreground cloud itself has a small filling factor and the individual foreground clumps are by chance distributed preferentially in front of the background clumps. For filling factors of $\alpha_f \lesssim 0.5$, our observations cannot be fitted with a single temperature model: this justifies our assumption that the filling factor of the foreground cloud is close to unity. One should keep in mind, however, the possibility that a multitemperature model might be necessary to represent the true physical environment in the cloud. High-resolution observations, in which variations of the absorption on small angular scales could be detected, will prove whether or not our assumptions indeed are valid for the cloud we observed.

The cloud parameters we derive are comparable to those derived from 492 GHz [C I] $^3P_1 \rightarrow ^3P_0$ emission observations of high-latitude translucent clouds with the AST/RO telescope (Ingalls et al. 1997). This indicates that we observe molecular clouds with physical properties similar to those clouds seen in emission toward high latitudes. The relatively large line width of $\sim 6 \text{ km s}^{-1}$ of the [C I] absorption indicates that we observe more than one cloud in the line of sight. We thus assume that our observations trace an average value for C I column densities of cold ($T_{\text{ex}} \leq 10 \text{ K}$) translucent clouds toward the inner disk of the Galaxy near the midplane.

In order to determine the fractional abundance of cold neutral carbon in the Galactic disk, we compare our derived parameters with the low-resolution spectral sky survey made with the COBE Far-Infrared Absolute Spectrometer (FIRAS) (Wright et al. 1991; Bennett et al. 1994), which traces emission from the warm component of interstellar neutral carbon. The [C I] $^3P_1 \rightarrow ^3P_0$ longitude cut along the Galactic plane in Bennett et al. (1994) is an average over $\pm 5^\circ$ in latitude and 5° in longitude around the Galactic equator. For longitudes $l \lesssim 30^\circ$, the integrated intensity is almost constant at $5 \times 10^{-7} \text{ ergs cm}^{-2} \text{ s}^{-1} \text{ sr}^{-1}$, except for a high peak toward the Galactic center itself. This intensity is equivalent to a velocity-integrated brightness temperature of 4 K km s^{-1} , a factor of about 5 higher than typical [C I] lines observed toward high-latitude clouds by Ingalls et al. (1997). The 810 GHz [C I] $^3P_2 \rightarrow ^3P_1$ integrated intensity of about $1.6 \times 10^{-6} \text{ ergs cm}^{-2} \text{ s}^{-1} \text{ sr}^{-1}$ (equivalent to a velocity-integrated brightness temperature of 2.9 K km s^{-1}) in the innermost $\pm 5^\circ$ of the Galaxy decreases even more steeply than does the 492 GHz intensity, to a value of about $4 \times 10^{-7} \text{ ergs cm}^{-2} \text{ s}^{-1} \text{ sr}^{-1}$ (equivalent to 0.7 K km s^{-1}) at $l \approx \pm 30^\circ$.

For the derivation of the optical depth and column densities consistent with both observed [C I] line fluxes from COBE, we follow the same method as described for the derivation of the excitation temperature of the absorbing cloud from ^{13}CO intensity ratios by applying equations (7)–(9). Assuming a typical line width of 10 km s^{-1} and LTE for both transitions in the entire COBE beam, a single-temperature fit of the observed flux in both transitions gives the following values for T_{ex} and the column density of C I: T_{ex} decreases from 22 K in the innermost $\pm 5^\circ$ in longitude with a column density of $1.1 \times 10^{17} \text{ cm}^{-2}$ to about 15 K with $6.5 \times 10^{16} \text{ cm}^{-2}$ at $l \approx \pm 30^\circ$. Note that these numbers are upper limits for the column density of C I in any possible multitemperature model in which all components have excitation temperatures higher than or equal to the single component model. The FWHM thickness of the molecular

cloud layer in the Galactic disk is $\sim 140 \text{ pc}$ (Bronfman et al. 1988). This converts to a thickness in latitude of $\sim 2^\circ$ at half the distance to the Galactic center, i.e., the main emission comes from latitudes $b \lesssim \pm 1^\circ$. Thus we assume a C I beam-filling factor for the COBE observations that is one-fifth the filling factor of the low-excitation absorbing gas we observe. We take the upper limit for the column density of C I toward $l \approx 30^\circ$ to be a typical value for the Galactic disk. On the line of sight to Sgr C, the upper limit for warm cloud material with $T_{\text{ex}} = 20 \text{ K}$ is then a factor of 2 smaller than the lower limit for the column density of the cold C I, derived from our absorption-line observations. If we assume that both the COBE $l = \pm 30^\circ$ data and the Sgr C line of sight are typical of the Galactic disk, a two-component model is needed. The relative brightness of the $^3P_2 \rightarrow ^3P_1$ and $^3P_1 \rightarrow ^3P_0$ (C I) lines in the COBE data indicates a component with $T_{\text{ex}} \gtrsim 15 \text{ K}$, whereas our absorption line data indicate a component with $T_{\text{ex}} \sim 5 \text{ K}$. There is no contradiction between the two data sets, because the $T_{\text{ex}} \sim 5 \text{ K}$ gas would not make a significant contribution to the brightness seen by COBE, even if the column density of the $T_{\text{ex}} \sim 5 \text{ K}$ gas is significantly higher than that of the $T_{\text{ex}} \gtrsim 15 \text{ K}$ gas.

It is not surprising that there is a considerable quantity of low-excitation atomic carbon in the Galactic plane. What is not known is to what degree these carbon atoms are associated with molecular, rather than atomic, hydrogen. It is possible that the present observations are an indication of significant translucent gas in the Galactic plane where the molecular hydrogen is associated with low-level $^3P_1 \rightarrow ^3P_0$ (C I) emission rather than with CO.

5. CONCLUSION

We have observed a deep $^3P_1 \rightarrow ^3P_0$ (C I) absorption feature with a width of $\sim 6 \text{ km s}^{-1}$ toward extended line emission near Sgr C. This feature is also visible in absorption in ^{13}CO at the same position. The line ratio of ^{13}CO $J = 1-0$ and $J = 2-1$ absorptions and the depth of the absorption in [C I] indicate that the absorbing material is extremely cold. We derive a [C I] excitation temperature of 5 K, at low volume densities, $n(\text{H}_2) \lesssim 10^3 \text{ cm}^{-3}$. A lower limit for the column density of cold C I is $3.5 \times 10^{17} \text{ cm}^{-2}$. The measured abundance ratio of C I to ^{13}CO is ~ 34 , and the abundance ratio of C I to ^{12}CO is ~ 1 , which is consistent with photochemical model calculations. The derived column density corresponds to an A_V of $\sim 4 \text{ mag}$.

If our observations represent the mean column density of a cold ($T_{\text{ex}} \leq 10 \text{ K}$) component of interstellar disk clouds, these clouds would only contribute a small fraction of the C I emission observed with COBE. Taking into account that our absorption observations give lower limits for the C I column density of an extremely cold component, whereas the column density of a warm ($T_{\text{ex}} > 20 \text{ K}$) component derived from COBE is an upper limit, we conclude that our observations give strong evidence that C I present in cold translucent clouds is a major component of the neutral carbon present in the Galactic disk. Because of its low excitation, this cold component is difficult to detect in emission.

We thank J. Bally for providing the Bell Labs data and J. Zmuidzinas and T. Phillips for the 492 GHz mixer used in the [C I] observations. We are grateful to the 1995 and 1996 South Pole Station crews and Antarctic Support Associates

for all their help. This research was supported in part by the National Science Foundation under a cooperative agreement with the Center for Astrophysical Research in Antarctica (CARA), grant number NSF OPP 89-20223. CARA is

an NSF Science and Technology Center. Research support was also provided by the Deutsche Forschungsgemeinschaft with grant number SFB 301 and by NATO Collaborative Research Grant No. 910495.

REFERENCES

- Bally, J. 1996, in ASP Conf. Proc. 102, *The Galactic Center*, ed. R. Gredel (San Francisco: ASP), 8
- Bally, J., Stark, A. A., Wilson, R. W., & Henkel, C. 1987, *ApJS*, 65, 13
- Bennett, C. L., et al. 1994, *ApJ*, 434, 587
- Bensch, F., Panis, J. F., Stutzki, J., Heithausen, A., & Falgarone, E. 1997, in preparation
- Bronfman, L., Cohen, R. S., Alvarez, H., May, J., & Thaddeus P. 1988, *ApJ*, 324, 248
- Chamberlin, R. A., Lane, A. P., & Stark, A. A. 1997, *ApJ*, 476, 428
- Engargiola, G., Zmuidzinas, J., & Lo, K.-Y. 1994, *Rev. Sci. Instrum.*, 65, 1833
- Flower, D. R., Le Bourlot, J., Pineau des Forêts, G., & Roueff, E. 1994, *A&A*, 282, 225
- Genzel, R. 1992, in *The Galactic Interstellar Medium*, ed. W. B. Burton, B. G. Elmegreen, & R. Genzel (New York: Springer), 275
- Goss, W. M. 1967, *ApJS*, 15, 131
- Hagen, J. P., Lilley, A. E., & McClain, E. F. 1955, *ApJ*, 122, 361
- Ingalls, J. G., Bania, T. M., & Jackson, J. M. 1994, *ApJ*, 431, L139
- Ingalls, J. G., Chamberlin, R. A., Bania, T. M., Jackson, J. M., Lane, A. P., & Stark, A. A. 1997, *ApJ*, 479, 296
- Lada, C. J., Lada, E. A., Clemens, D. P., & Bally, J. 1994, *ApJ*, 429, 694
- Lane, A. P., & Stark, A. A. 1996, *Antarctic J. of the US*, 30(5), 377
- Lasenby, J., Lasenby, A. N., & Yusef-Zadeh, F. 1989, *ApJ*, 343, 177
- Liszt, H., Sanders R. H., & Burton, W. B. 1975, *ApJ*, 198, 537
- Lucas, R., & Liszt, H. 1994, *A&A*, 282, L5
- Meixner, M., & Tielens, A. G. G. M. 1993, *ApJ*, 405, 216
- Nussbaumer, H. 1971, *ApJ*, 166, 411
- Penzias, A. 1980, in *IAU Symp. 87, Interstellar Molecules*, ed. B. H. Andrew (Dordrecht: Reidel), 397
- Phillips, T., & Huggins, P. J. 1981, *ApJ*, 251, 533
- Röhrig, R. 1995, in *Das KOSMA-Observatorium und seine Hardware*, Technical Report, Univ. of Cologne
- Schilke, P., Keene, J., Le Bourlot, J., Pineau des Forêts, G., & Roueff, E. 1995, *A&A*, 294, L17
- Snyder, L. E., Buhl, D., Zuckermann, B., & Palmer, P. 1969, *Phys. Rev. Lett.*, 22, 679
- Staguhn, J., Stutzki, J., Yusef-Zadeh, F., & Uchida, K. I. 1997, *A&A*, submitted
- Stark, A. A., Chamberlin, R. A., Cheng, J., Ingalls, J., & Wright, G. 1997, *Rev. Sci. Instrum.*, 68, 2200
- Stark, R., & van Dishoeck, E. F. 1994, *A&A*, 286, L43
- Stark, R., Wesselius, P. R., van Dishoeck, E. F., & Laureijs, R. J. 1996, *A&A*, 311, 282
- Stutzki, J., Stacey, G. J., Genzel, R., Harris, A. I., Jaffe, D. T., & Lugten, J. B. 1988, *ApJ*, 332, 379
- van Dishoeck, E. F., & Black, J. H. 1988, *ApJ*, 334, 771
- . 1989, *ApJ*, 340, 273
- van Dishoeck, E. F., Blake, G. A., Draine, B. T., & Lunine, J. I. 1993, in *Protostars and Planets III*, ed. E. H. Levy & J. I. Lunine (Tucson: Univ. of Arizona Press), 163
- Winnemisser, G., et al. 1986, *A&A*, 167, 207
- Wright, E. L., et al. 1991, *ApJ*, 381, 200
- Zmuidzinas, J., & Le Duc, H. G. 1993, *IEEE Trans. Microwave Th. Tech.*, 40, 1797